



## **Ordnance Heating Rates in Shipboard Magazines**

Con Doolan

DSTO-TR-1188

**DISTRIBUTION STATEMENT A**  
Approved for Public Release  
Distribution Unlimited

20011203 206

# Ordnance Heating Rates in Shipboard Magazines

*Con Doolan*

**Weapons Systems Division  
Aeronautical and Maritime Research Laboratory**

DSTO-TR-1188

## **ABSTRACT**

This report describes a numerical method of determining the heating rate to ordnance cylinders stored in a Ship's Magazine. The source of heating is assumed to be a hydrocarbon fuel fire burning in an adjacent compartment. The heat released from the fire raises the temperature of a common bulkhead which then radiates energy onto the ordnance in the magazine. The method compares well with data available in the literature for shipboard fuel fire. Based on the strength of these comparisons, the method is used to estimate the likely heating rate for the Penguin ASM while mounted within the ANZAC Air Weapons magazine.

## **RELEASE LIMITATION**

*Approved for public release*

DEPARTMENT OF DEFENCE  
DEFENCE SCIENCE & TECHNOLOGY ORGANISATION | **DSTO**

AQ F02-02-0340

*Published by*

*DSTO Aeronautical and Maritime Research Laboratory  
506 Lorimer St  
Fishermans Bend Vic 3207 Australia*

*Telephone: (03) 9626 7000*

*Fax: (03) 9626 7999*

*© Commonwealth of Australia 2001*

*AR-011-953*

*July 2001*

**APPROVED FOR PUBLIC RELEASE**

# Ordnance Heating Rates in Shipboard Magazines

## Executive Summary

Fire near or within shipboard magazines is a potent threat to ship survivability. Information on the time-to-reaction of ordnance stored within ship magazines is of vital importance for fire-fighters, ship commanders and Naval planners as cookoff reactions (the ordnance reaction which occurs when heat is applied for a period of time) are of sufficient violence to cause a high number of fatalities and loss of platforms. Standard methods for assessing weapons systems during slow cookoff are experimental and are therefore expensive as they require the destruction of a complete munition. Determination of a suitable slow cookoff heating rate is also difficult to determine as rates are specific to the particular accident or combat scenario.

This report presents a numerical model which enables the determination of reliable radiative heat transfer rates for ordnance stored in a shipboard magazine when there is a fire in an external compartment. The model uses an explicit formulation of the heat transmission equations and some approximations for absorption and radiation of the sooty gas within the magazine. Results from the model are compared with experimental results obtained from the open literature. The results are in reasonable agreement indicating that the model provides heating rate results which are of suitable accuracy for time-to-reaction calculations. Results are also presented for the Penguin rocket motor situated in various positions within the Anzac Air Weapons Magazine. Two fire scenarios are considered which give a broad range of heating rate levels indicating that the peak heating rate is highly dependant of the distance between the missile and the heated wall.

The numerical model developed in this report can now be used with finite element software for the determination of time-to-reaction during cookoff of complete weapon systems. This represents the next stage in the project for Weapons Systems Division. This will provide Navy with valuable information and also reduce the requirement for full scale munitions testing.

## Authors

### **Dr Con Doolan** Weapons Systems Division

*Dr Con Doolan graduated from the University of Queensland in 1992 with a Bachelor of Mechanical Engineering. He later conducted research on hypervelocity wind tunnels and was awarded a Doctor of Philosophy in 1997. Dr Doolan joined DSTO in 2000 after working at the University of Glasgow on helicopter aerodynamics. He now performs research on missile propulsion systems for the ADF and has interests in rocket motor insensitive munitions response and advanced propulsion systems.*

---

# Contents

1. INTRODUCTION .....	1
2. NUMERICAL MODEL.....	2
2.1 Heat Transfer Modelling.....	3
2.2 Fire Compartment model .....	4
2.3 Heat Transfer Relations.....	5
2.4 Soot Production and Magazine Heat Transfer.....	6
2.5 Heating Rate of Ordnance Cylinders.....	8
2.6 Comment on Numerical Procedure .....	9
3. COMPARISON WITH EXPERIMENTAL RESULTS FROM THE LITERATURE. 9	
3.1 ex-USS <i>Shadwell</i> Results .....	10
3.1.1 Model Set Up.....	10
3.1.2 Comparison with Phase III Results.....	11
3.1.3 Comparison with Phase IV Results.....	13
3.2 MAYO-LYKES Results .....	15
3.2.1 Model Set Up.....	15
3.2.2 Comparison with Experimental Results .....	17
3.3 Summary.....	20
4. CALCULATION OF ORDNANCE HEATING RATES IN THE ANZAC AIR WEAPONS MAGAZINE .....	20
4.1 Test Case 1: Fire in Refuelling Compartment .....	23
4.2 Test Case 2: Fire in Hangar Space .....	27
5. CONCLUSIONS AND FUTURE WORK.....	30
6. REFERENCES.....	31
APPENDIX A: SHAPE FACTOR EQUATIONS .....	33

# 1. Introduction

Naval crews live and work amongst explosive ordnance. It is therefore crucial that a proper understanding of how energetic material behaves when exposed to unplanned stimuli such as mechanical impact or heat be gained. Of particular importance here is the reaction of ordnance to heat. The application of heat to energetic material results in (heat releasing) thermal decomposition reactions which occur within these materials. Eventually the material reaches a temperature where the thermal decomposition becomes self-sustaining and thermal run-away occurs. This generally starts a deflagration process which builds to a violent reaction such as explosion or detonation. The application of heat to energetic material for sufficient time for reaction to occur is generally known as "cookoff". For obvious reasons, knowledge of the cookoff time-to-reaction is important for those responsible for fighting fires near or within shipboard magazines.

Much work has been done in measuring cookoff time-to-reaction and the violence of response. These tests are generally done using full scale munitions or a cookoff "bomb" arrangement where a small sample is encased in a steel tube and heated using expendable band heaters. These tests use standard heating rates defined in the US military standard MIL-STD-2105B or another heating rate thought appropriate. The heating rates are divided into fast and slow values. The fast heating rate is achieved by exposing the munition directly to a hydrocarbon pool fire or wood based bonfire in accordance with the relevant standard. This type of testing is unambiguous as it clearly simulates the case where the weapon is immersed in fire. The definition of a realistic slow heating rate is more difficult to achieve. Slow heating rates apply to all situations where heat can be applied by means other than the direct exposure to a fuel fire. This involves a very large number of heating rates each applicable to its own scenario. The standard heating rate of 3.3 K/hr listed in MIL-STD-2105B is very low and can result in reaction times measured in days. Some researchers use an intermediate heating rate of 27.8 K/hr (Victor 1995) in an effort to define a more realistic heating rate.

In the absence of specific experimental data, determination of the likely slow heating rate ordnance will experience in an operational environment requires direct modelling of the particular scenario. In the present work it is of interest to estimate the heating rates experienced by munitions in a shipboard magazine due to fire in an adjacent compartment. In such a scenario, the fire heats a common bulkhead which then heats objects in the magazine by direct radiation. The heated air within the magazine also radiatively and convectively heats the munition. Once the ordnance heating rates are determined, time-to-reaction modelling and experimentation can be performed in order to give ADF commanders and planners realistic information for operational issues such as fire-fighting response times or evacuation times.

This report presents a numerical method of determining ordnance heating rates in a shipboard magazine due to an external fire. Section 2 describes the numerical method used to determine the heating rates. Section 3 compares results obtained using the method with data available in the literature. Section 4 then presents results using the code for the penguin missile in the Anzac Air Weapons Magazine. The report is concluded in Section 5.

## 2. Numerical Model

The determination of ordnance heating rates in a shipboard magazine due to an external fire is dependent on a number of factors. These include fire size and energy release rate, radiative and convective heat transfer properties, magazine and other compartment dimensions, bulkhead thickness, orientation of the ordnance in the magazine and soot production within the magazine due to decomposition of composites and paint. Considering the large number of parameters which influence heat transfer to munitions, any numerical model needs to be reasonably quick and robust. For this reason an explicit formulation of the transient heat transmission equations has been utilised along with certain assumptions which will be described below.

Previous modelling attempts for magazine heating rates have been performed by Mansfield (1996). The model presented below is similar to Mansfield's model and utilises some of the key assumptions in that work. Where Mansfield used the model to identify the major factors affecting ordnance heating rates, the model is extended and compared with experimental results in the literature.

Computational fluid dynamics modelling of shipboard fires in a break-bulk freighter has been performed by Koski et al. (1997b). Radiative and convective heat transfer were included in their model and it modelled the radiation to a cylindrical calorimeter in a hold adjacent to the fire compartment. The modelling therefore simulates a similar situation to the one considered in this report. However the computational time required to resolve the natural convection flow patterns in conjunction with the radiation and convection heat transfer was over 80 hours to simulate 25 minutes of shipboard fire time. This model did not include combustion modelling but releases energy at a predetermined rate to simulate a fire. The numerical model described in this report provides the essential data for ordnance heating using significantly less computational resources because the model does not couple the Navier-Stokes equations with radiative heat transfer. It is assumed that radiative heat transfer dominates the shipboard fire environment and convection provides only a modest level of heating. Indeed, the same conclusion was reached by Koski et al. (1997b) when they eliminated the convective heat transfer terms in their modelling.



## 2.1 Heat Transfer Modelling

The system is divided into a number of elements which have the ability to absorb or emit heat. An element can be a steel bulkhead, deck or overhead or can be the mass of gas contained within a compartment or magazine. The model is centred around the fire compartment which contains the hydrocarbon fuel fire. Up to six compartments may be arranged around the fire compartment, one of which is the magazine (Fig. 1). The remaining five compartments are used as heat sinks to account for heat losses out of the fire compartment. The dimensions of each of the compartments can be set independently in the model however, in naval design, it is usual to have a common bulkhead of similar dimensions between two compartments. This simplifies the analysis procedure. In some situations, one of the fire compartment walls forms part of the outer bulkhead. In this case, the additional compartment is replaced by a 298 K constant temperature boundary condition thereby simulating the ambient conditions outside.

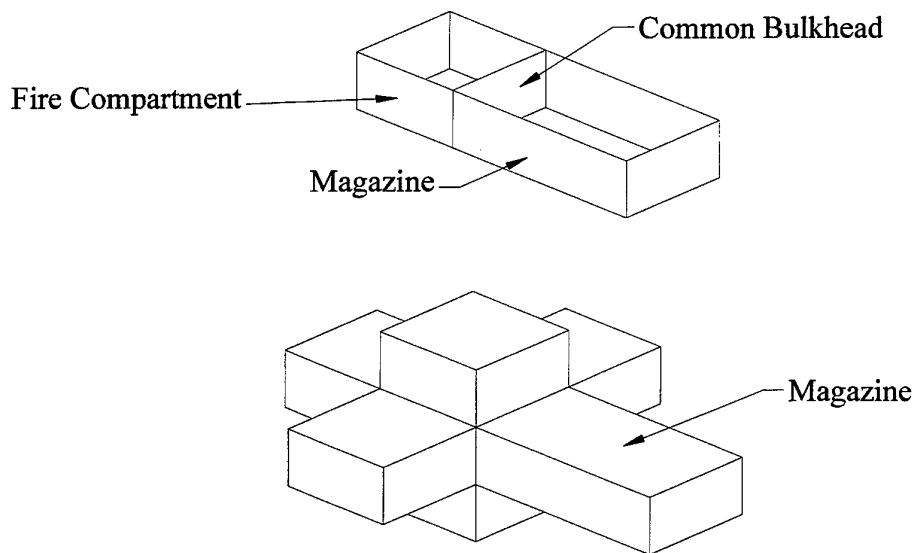


Figure 1. Compartment layout used for heating analysis.

Heat transfer is modelled using a simplified approach to the transient heat conduction problem. An energy balance method (Croft and Lilley 1977) has been used,

$$\frac{dT}{dt} = \frac{\sum Q}{mC_p} \quad (1)$$

where  $T$  is the temperature of the particular element (e.g. bulkhead, gas volume),  $t$  is the time,  $Q$  represents the heat transfer to or from the element from a particular source,  $m$  is the mass of the element and  $C_p$  is the specific heat of the element. The numerator represents the sum of all heat transfer (net heat transfer) to the element. Therefore, the procedure for solution consists of calculating the amount of net heat transfer to each element at each time step and then incrementing the temperature using Equation 1.

The net heat transfer consists of radiation from gas and steel bulkheads, decks and overheads and also from convection from the gases within each compartment. The fire is modelled as a heat release into the fire compartment gas.

## 2.2 Fire Compartment model

The fire is modelled as an energy release directly into the fire compartment gas. A simplified approach (Mansfield 1996) to the fuel energy release rate ( $Q_f$ ) is to assume it is directly proportional to the evaporation mass flux of the fuel ( $\rho_f V_f$ ), the surface area of the fire ( $A_f$ ) and the heat of combustion of the fuel ( $H_c$ ),

$$Q_f = \rho_f V_f A_f H_c \quad (2)$$

The evaporation mass flux is assumed constant for most of the burn period. Its value can be estimated from hydrocarbon pan fire testing in the literature. It is defined as the mass flow rate of fuel consumed by the fire divided by the surface area of the burning surface. Table 1 compares the evaporation mass flux determined from various sources.

Table 1. Comparison of calculated fuel evaporation rates from various sources.

Fuel	$\rho_f V_f$ (kgm <sup>-2</sup> s <sup>-1</sup> )	Reference
Jet - A1	0.069	Holbrook and Cawley (1986)
Heptane	0.048	Durkin et al. (1993)
JP4	0.099	Johnson et al. (1982)
Diesel	0.044	Koski et al. (1997a)
'General Hydrocarbon'	0.062	Mansfield (1996)

The heat of combustion for the various hydrocarbons was determined from Rossini et al. (1953).

It is assumed that steady state conditions prevail during combustion and the total mass of gas within the fire compartment remains constant throughout the burning period. It is realised that actual flame densities can vary greatly depending on local temperature and pressure values however, as this model assumes a constant mass of gas within the fire compartment, a constant density of 1.44 kgm<sup>-3</sup> is used, following the numerical modelling procedure of Mansfield (1996). Unlike other heat transfer models, density

affects the mass only and is decoupled from the heat transfer coefficients which are specified independently. A constant specific heat of  $1402 \text{ J kg}^{-1} \text{ K}^{-1}$  was also assumed.

Uniform temperature of the combustion products is a simplification of the actual processes occurring, however the alternative is a much more computationally expensive algorithm which in itself may contain many uncertainties. It will be shown that the assumption of uniform gas temperature yields results which compare favourably with experimental values. Heat losses within the fire compartment are modelled as radiative and convective losses through the bulkheads. Other heat losses may occur due to incomplete combustion, turbulent mixing of cold input air and energy losses through the exhaust port. A combustion 'efficiency' factor is used to account for these additional heat losses. It is assumed that 75% of the heat released by combustion is available to heat the fire compartment gas.

## 2.3 Heat Transfer Relations

Thermal radiation from the hot combustion products in the fire compartment is assumed to follow the Stefan-Boltzman law,

$$Q = \varepsilon \sigma T_G^4 \quad (3)$$

where  $\varepsilon$  is the emissivity,  $\sigma$  is the Stefan-Boltzman constant and  $T_G$  is the gas temperature. It is assumed that the emissivity of the combustion products is unity thereby modelling a very sooty flame and gas. The amount of soot contained within the hydrocarbon flame depends on a number of factors, however is assumed to be unity here in order to simplify the model.

A similar expression is used for radiation from the walls (inside and outside the fire compartment) where the gas temperature is substituted for the wall temperature ( $T_w$ ). Emissivity is assumed to be 0.8 for naval/shipboard walls. This was estimated from the results of Koski et al. (1997a) who measured the emissivity of paint flakes removed from the bulkheads of a break-bulk freighter.

Equation 3 is also used for radiation from the magazine gas however the emissivity is modified to account for suspended carbon particles from decomposing organic materials and smoke. This is discussed in more detail in the next section.

There is also heat transfer to the walls by convection from the gases in contact with them. The general expression for the convective heat transfer is,

$$Q = h(T_G - T_w) \quad (4)$$

Where  $h$  is the convective heat transfer coefficient. The value of  $h$  varies depending on the gas medium and convective flow properties. Within the fire compartment  $h = 2.72$

Wm<sup>-2</sup>K<sup>-1</sup>. Within the air filled magazine and other compartments  $h = 2.04 \text{ Wm}^{-2}\text{K}^{-1}$  (Mansfield 1996).

## 2.4 Soot Production and Magazine Heat Transfer

As the fire heats the common bulkhead between the fire compartment and the magazine, the hot bulkhead radiates energy into the magazine space. While this energy heats the ordnance and is absorbed by the air, it also heats any organic material such as composite components or paint. The increase in temperature accelerates the decomposition of these products and at sufficiently high temperature they will form soot which disperses into the air. Also, exhaust from the neighbouring fire compartment may find its way into the magazine space and contribute to the soot density in the air. The dispersed carbon particles increase the effective absorptivity and emissivity of the air and therefore a higher proportion of radiation is emitted from the air to the ordnance. It is therefore important to include this effect in the numerical model.

It is difficult to evaluate with a high degree of confidence the soot production with time within the magazine. Indeed, it would depend significantly on the quantities of organic material actually present within the magazine and the leakage of smoke from the fire compartment which may be difficult to quantify. Characterisation of the decomposition reactions is also problematic with the chemical kinetic information for the various organic compounds being unknown or very complex.

In order to include the effects of dispersed soot, a simplified approach has been taken. It is assumed that a constant radiation absorption coefficient ( $a$ ) can be used for the magazine air. It will be shown in Section 3 that a value of  $a = 0.01 \text{ m}^{-1}$  gives good agreement with measured values. In crude terms, this value corresponds to a visibility where the human eye cannot see across an average sized room (Mansfield 1996). Assuming the absorption coefficient applies to all wavelengths, the transmissivity ( $\tau$ ) and absorptivity ( $\alpha$ ) can be calculated between each wall in the magazine using the relations (Holman 1981),

$$\begin{aligned}\tau_{i,j} &= e^{-ad_{i,j}} \\ \alpha_{i,j} &= 1 - \tau_{i,j}\end{aligned}\tag{5}$$

Where  $d$  is the distance between walls and the subscripts refer to the coefficients which apply between walls  $i$  and  $j$  within the magazine. The amount of energy absorbed by the magazine gas by radiation from the common bulkhead (wall 1) to the remaining five walls is therefore,

$$Q_{abs} = \sigma T_1^4 (F_{1,2}\alpha_{1,2} + F_{1,3}\alpha_{1,3} + \dots + F_{1,6}\alpha_{1,6})\tag{6}$$

where  $F_{ij}$  is the radiation shape factor between walls  $i$  and  $j$ . Similar expressions can be obtained for the energy absorbed by the gas by radiation from the other walls. The energy transmitted by radiation from five walls to the common bulkhead is,

$$Q_{trans} = \sigma (T_2^4 F_{2,1} \tau_{2,1} + T_3^4 F_{3,1} \tau_{3,1} + \dots + T_6^4 F_{6,1} \tau_{6,1}) \quad (7)$$

Again, similar expressions can be written for radiation transmitted to the other walls in the magazine. The shape factors between the magazine walls can be evaluated using the theory in Hottel and Sarofim (1967) which is incorporated into the numerical model. The equations for the shape factors are listed in Appendix A.

To calculate the emissivity of the magazine gas the theory of Stull and Plass (1960) is used. In this work monochromatic emissivity data is presented for dispersed carbon for the wavelength interval 0.4 to 20  $\mu\text{m}$  which covers the infrared and visible portions of the spectrum. Experimental data for certain flames (Stull and Plass 1960) shows that carbon particle densities can vary between  $10^{10}$  and  $10^{11} \text{ cm}^{-3}$  and have a mean radius of 200  $\text{\AA}$ . For the present work, it is assumed that the soot (carbon) particle density is  $10^{11} \text{ cm}^{-3}$  with an asymmetric distribution of particle sizes from 50 to 1000  $\text{\AA}$ . The total emissivity of the magazine soot/gas cloud can then be calculated from the monochromatic values using an integral procedure which is described below.

The total emissive power of the soot/gas cloud is,

$$E = \int_0^{\infty} \epsilon_{\lambda} E_{b\lambda} d\lambda \quad (8)$$

where  $\epsilon_{\lambda}$  is the monochromatic emissivity for wavelength  $\lambda$  and  $E_{b\lambda}$  is the emissive power of a black body per unit wavelength which can be written as (Holman 1981),

$$E_{b\lambda} = \frac{C_1 \lambda^{-5}}{e^{C_2/\lambda T} - 1}$$

$$C_1 = 3.743 \times 10^8 \text{ W}\mu\text{m}^4 \text{ m}^{-2} \quad (9)$$

$$C_2 = 1.4387 \times 10^4 \mu\text{mK}$$

where wavelength  $\lambda$  is in  $\mu\text{m}$ . The total emissivity can then be calculated by dividing the total emissive power by the emissive power of a black body at the same temperature as the soot/gas cloud,

$$\epsilon = \frac{E}{\sigma T^4} \quad (10)$$

To calculate the total emissive power using the data of Stull and Plass (1960), a first order numerical integration of the monochromatic emissivity data was performed. As the data is

limited to the infrared and visible portions of the spectrum, the method is only valid for radiation in this range. Fortunately this limits the method to a temperature well above the calculated maximums of approximately 600-700 K in the present work.

A subroutine has been incorporated into the numerical model which calculates the total emissivity of the magazine gas at each time step.

## 2.5 Heating Rate of Ordnance Cylinders

Now that the method of calculating heat transfer to the common bulkhead and magazine gas has been determined, the heating rate to the stored ordnance can now be calculated. Figure 2 shows a schematic of an arrangement of an ordnance cylinder (e.g. missile, torpedo) placed parallel to the common bulkhead which is heated by a fire in the adjacent compartment. The radiative heat load to the ordnance consists of a uniform radiation from the hot magazine gas and also a non-uniform radiation from the hot common bulkhead. Radiation loads from the other magazine walls are not considered significant due to their low temperatures.

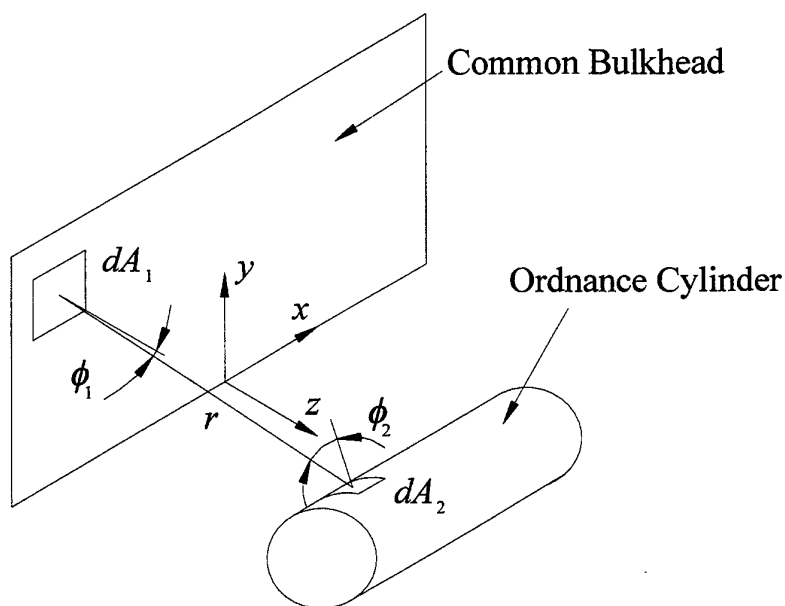


Figure 2. Schematic showing ordnance cylinder parallel to radiating bulkhead.

To determine the non-uniform heating rate distribution due to radiation from the common bulkhead the following approach is followed. The common bulkhead is discretised into 2500 equal elemental areas. The net thermal radiation between any two elements  $dA_1$  and  $dA_2$  can be calculated using the following relation (Holman 1981),

$$dq_{1 \rightarrow 2} = \varepsilon_w \sigma (T_w^4 - T_s^4) \cos \phi_1 \cos \phi_2 \frac{dA_1 dA_2}{\pi r^2} \quad (11)$$

where  $T_w$  is the common bulkhead temperature,  $\varepsilon_w$  is the emissivity of the common bulkhead,  $T_s$  is the surface temperature of the ordnance at  $dA_2$  and the other symbols are defined in Fig. 2. The angles,  $\phi_1$  and  $\phi_2$ , are measured relative to the normal from each respective surface. The heat transfer per unit area at a point on the ordnance cylinder due to the radiation from  $dA_1$  can be determined by dividing both sides of Eq. 11 by  $dA_2$ . To calculate the total heating rate at a point on the ordnance cylinder it is necessary to sum the components from each element on the bulkhead (or integrate in the limit  $dA_1 \rightarrow 0$ ). This can be done for any point on the ordnance cylinder and is calculated in the numerical model at 200 locations around the circumference of a section through the ordnance cylinder.

Calculation of the radiation from the magazine gas is a straight-forward process using the total emissivity and the gas temperature with the Stefan-Boltzman law for radiation.

## 2.6 Comment on Numerical Procedure

The numerical procedure is essentially a one dimensional representation of the heat transfer mechanisms. A fixed time step between 0.25 and 1.0 s was used for all calculations presented in this report. To test the suitability of these time steps, a number of test runs were performed using time steps reduced by up to 50%. It was found that the post run gas and bulkhead temperatures after 45 minutes of burning varied by a maximum of 0.04% and hence it was concluded that the model was time step independent when operating at with a time step of 1.0 s or below.

## 3. Comparison with Experimental Results from the Literature

In order to have confidence in the numerical model's ability to predict ordnance heating rates, computational results have been compared with experimental results from the literature. Fortunately, there are a number of shipboard fire experiments where the concern has been heat transmission from the fire compartment into adjacent holds. Three experiments reported in the literature are used to test the computational fire and heat transfer model. Two of these experiments were performed on the ex-USS *Shadwell*, a Naval Research Laboratory (U.S.A.) test ship (Williams et al. (1993) and Durkin et al. (1993)). These experiments measured fire compartment gas temperatures along with wall and air temperatures in the hold adjoining the fire compartment. The two experiments are designated Phase III and Phase IV and this nomenclature will be maintained in this report.

The third series of experiments are reported by Koski et al. (1997a, 1998) on the break-bulk freighter *MAYO-LYKES* where cylindrical calorimeters were placed next to a common bulkhead, heated on one side by a variety of fire scenarios. The calorimeters were meant to simulate radioactive packages which experience a fire during shipment. The calorimeters used were of a fortunate design which allows direct comparison of heating rate results to those calculated using the model described in this report.

### **3.1 ex-USS *Shadwell* Results**

#### **3.1.1 Model Set Up**

The experimental arrangement was the same for both the Phase III and Phase IV results. The tests were performed on the port wing of the *Shadwell*. The fire was initiated in a compartment labelled Berthing 2. The adjacent compartment which can be considered analogous to the magazine in the model is an overhead compartment known as RICER 2. Therefore, in this situation, the common bulkhead is the overhead of Berthing 2 or deck of RICER 2. The geometry used to model the *Shadwell* tests is shown in Fig. 3. The model shows the fire compartment (Berthing 2) and the effective magazine (RICER 2) and the common wall. As the tests were performed on the port wing, one of the compartments adjacent to the fire has been removed and replaced with a constant gas temperature boundary condition (298 K) simulating the outside temperature. Four additional compartments are arranged around the fire compartment simulating the adjoining areas of the ship. All compartments are of identical size and all walls are 9.7 mm (0.38 in) thick steel with no insulation.



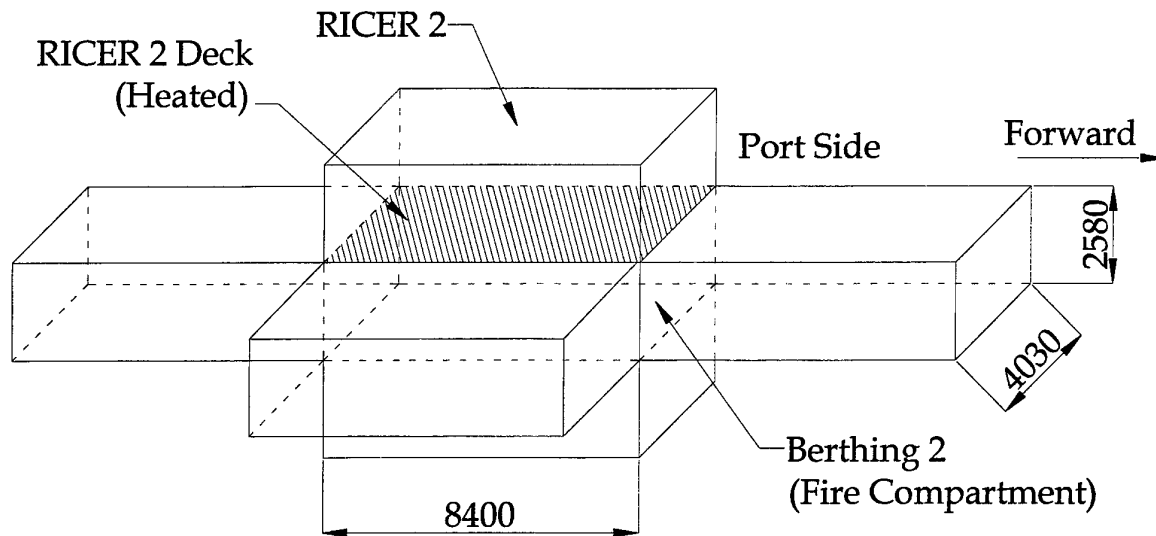


Figure 3. Schematic of ex-USS Shadwell model set up, dimensions in millimetres.

A post-flashover fire was experimentally simulated by using a diesel spray fire in Berthing 2. Three steel pans (each 1.2 m x 1.2 m) and 0.102 m deep were placed on the deck of Berthing 2. Heptane was poured into each of the pans and ignited simultaneously and allowed to burn almost to completion (2.5 minutes after ignition). Diesel fuel was then sprayed across the hot pans which ignited the diesel fuel instantaneously. The total diesel fuel flow rate from the spray nozzles was 17.4 Litres-per-minute. The estimated heat release rate from the diesel spray fire is 9.2 MW if a heat of combustion of 37.77 MJkg<sup>-1</sup> is assumed.

The fire is modelled in two stages. The first simulates a heptane pool fire which burns for 2.5 minutes. The fuel evaporation rate was determined from the tests and the value can be found in Table 1. The second stage simulates the diesel fuel fire immediately after the heptane by releasing 9.2 MW of energy for a further 20 minutes.

The numerical model is compared with gas temperature measurements within the fire compartment (Berthing 2), the common wall temperature (RICER 2 deck) and the air temperature inside the effective magazine (RICER 2).

### 3.1.2 Comparison with Phase III Results

The Phase III tests were concerned with venting the Berthing 2 and RICER 2 compartments and the effect on the heat transfer to the air within RICER 2. The aim of

the tests was to gain information for Naval fire fighters. Results were obtained for various venting cases, including the situation where the RICER 2 compartment was sealed. The results from the sealed RICER 2 test case are used to compare with the numerical model. It should be noted that venting of RICER 2 did not significantly alter the transient temperature rise of the air.

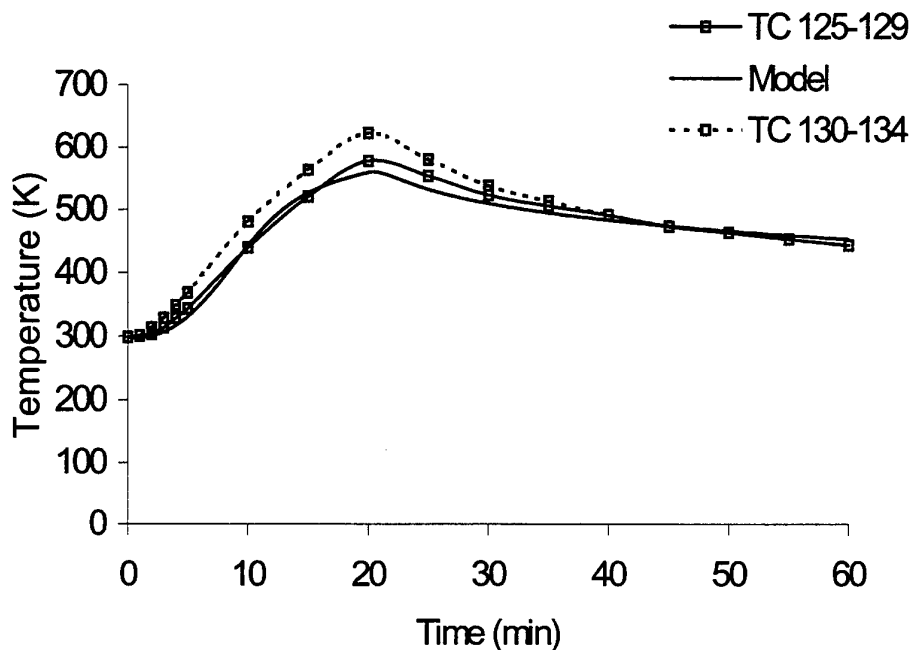


Figure 4. Comparison of model with ex-USS Shadwell Phase III experimental results for RICER 2 air temperature.

Figure 4 shows a comparison between the numerical model and the experimental data for the air temperature within RICER 2. A constant absorption coefficient of 0.01 for the magazine gas was used for this test. The average for two thermocouple trees are shown (labelled TC 125-129 and TC 130-134). The thermocouple trees are placed at different locations within the RICER 2 compartment and give an indication of the temperature variation across the compartment. The model compares well against the experimental data for the first 17 minutes of the test. The peak temperature at 20 minutes (the point where the fuel is shut off) is slightly under-predicted. After the fuel is turned off, temperature loss rates are approximately the same, indicating that thermal heat losses are modelled correctly.

### 3.1.3 Comparison with Phase IV Results

Data available from the Phase IV tests are more extensive and provide more detailed information about gas and wall temperatures. These tests were concerned with evaluating various forms of thermal insulation for the U.S. Navy. The insulation was mounted in small test areas on the RICER 2 deck. For comparison with the numerical model, the effects of the insulated portions of the deck was considered insignificant as only a small portion of the deck area was covered.

Figure 5 compares the measured Berthing 2 (fire compartment) gas temperatures with the numerical model. Each experimental curve represents the average of three thermocouples mounted on a thermocouple tree at the same location in Berthing 2. The experimental curve is also the average of five fire tests. The results indicate the spatial variation in gas temperature during the experiment as the thermocouple trees are widely spaced within Berthing 2. The computed result lies between the two experimental curves, indicating reasonable agreement. The model significantly over-predicts the gas temperature during the early portion of the curve when the heptane pool fire is burning. This discrepancy cannot be accounted for, however it does not seem to affect the comparisons with the results in the adjacent compartment (RICER 2).

Figure 6 compares the measured RICER 2 deck temperature with the model. The experimental results are an average of seven thermocouples placed at various locations on the bare steel deck, giving an average deck temperature with time. These data are for a single test. The model compares very well with the experimental results in the first half of the simulation, despite the early differences in the Berthing 2 gas temperatures shown in Fig. 5. After this point, the model begins to marginally over-predict the experimental bulkhead temperature. The maximum discrepancy is 6.3%.

Figure 7 compares the measured RICER 2 air temperature with the numerical model. The model slightly under-predicts the experimental air temperature however the agreement can be considered good. This confirms the result obtained for the Phase III tests and gives further confidence in the value selected for the absorptivity coefficient (0.01).

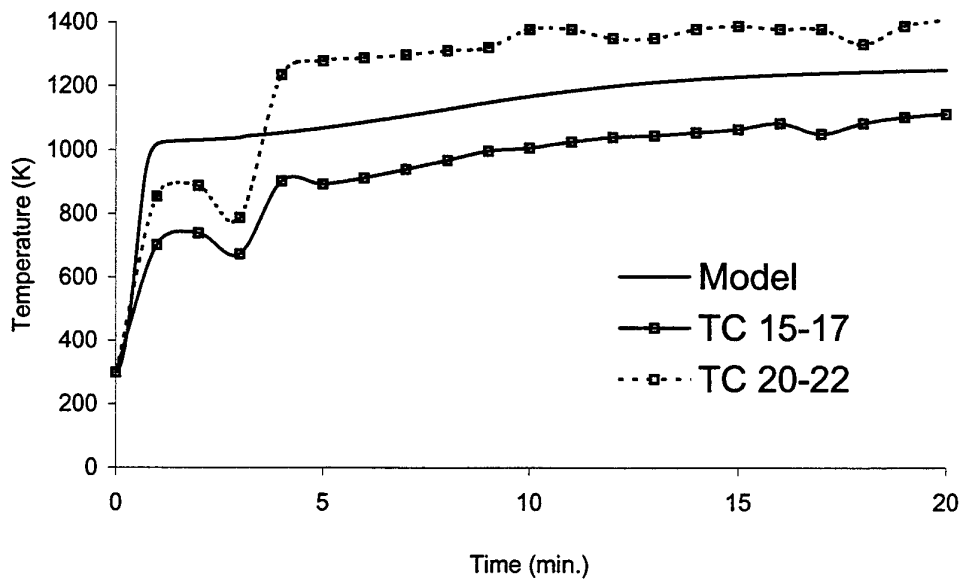


Figure 5. Comparison between numerical model and Berthing 2 Gas Temperatures for ex-USS Shadwell Phase IV tests.

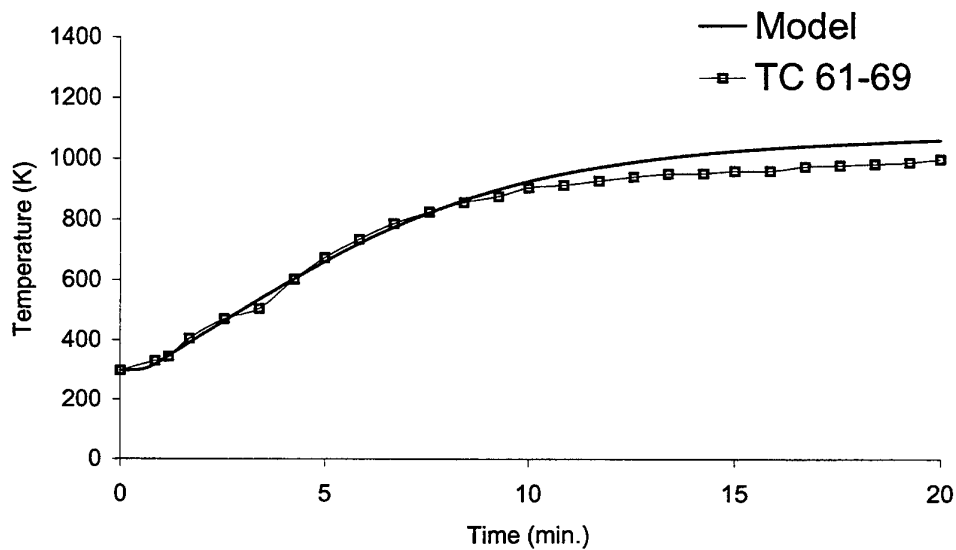


Figure 6. Comparison between numerical model and RICER 2 deck temperatures for ex-USS Shadwell Phase IV tests.

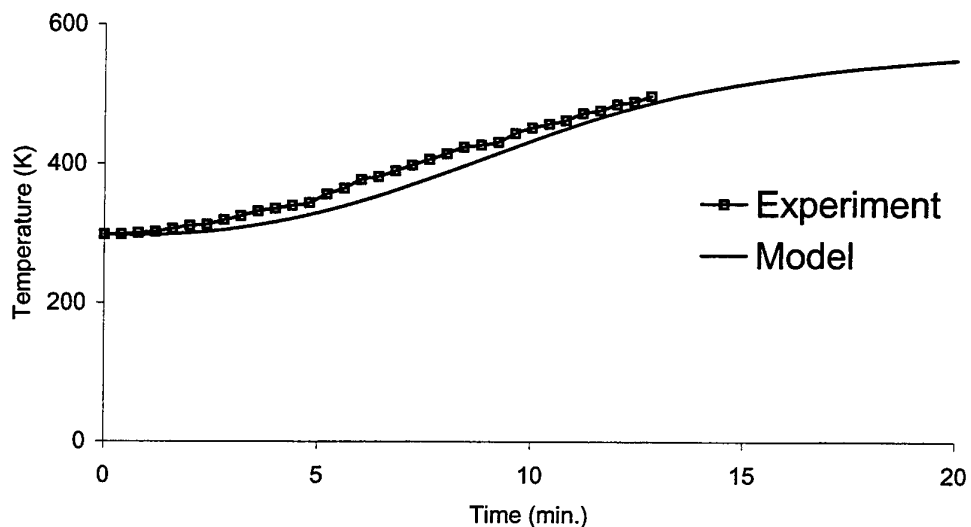


Figure 7. Comparison between experimental RICER 2 air temperature and numerical model for ex-USS Shadwell Phase IV tests.

### 3.2 MAYO-LYKES Results

#### 3.2.1 Model Set Up

Sandia National Laboratories performed a series of tests to determine the heat transfer to simulated radioactive cargo packages during a shipboard fire. To do this they performed a number of experiments aboard a break-bulk freighter, the *MAYO-LYKES*. The experiments were performed in two holds within the freighter, where a fire was started in one hold and instrumentation was placed at many locations in each hold. Of particular relevance here is the simulated radioactive package. The package was simulated experimentally as a cylindrical calorimeter, placed parallel to the common bulkhead. This is very fortunate for the purposes of validating the present numerical model. The experimental geometry used for the experiments can very easily be modelled using the numerical code.

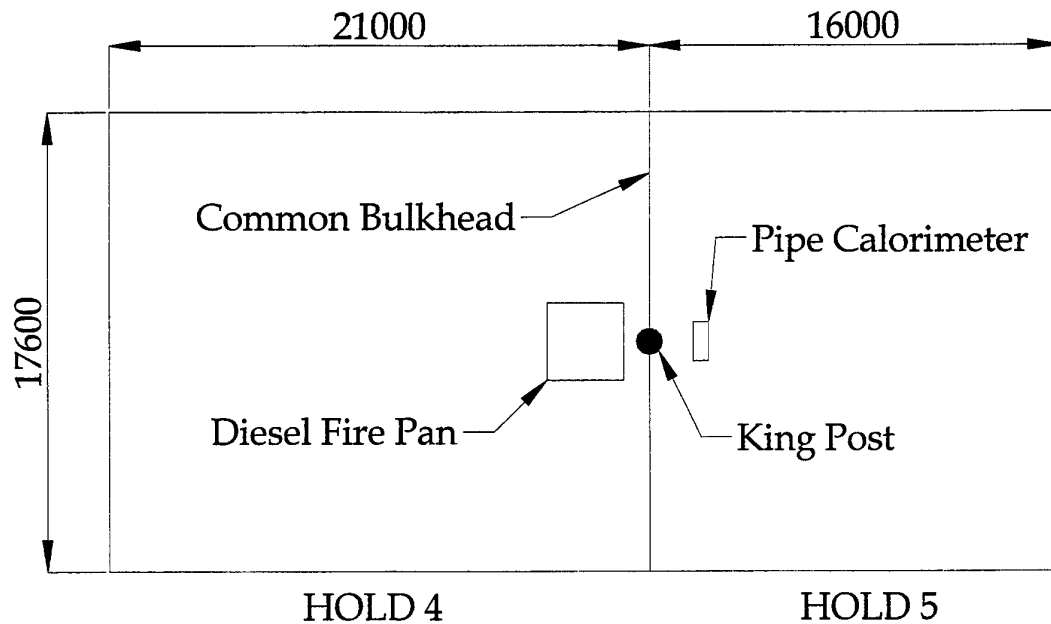


Figure 8. Plan View of MAYO-LYKES model setup, dimensions in millimetres.

Figure 8 shows a plan view of the geometry used to model the MAYO-LYKES experiments. The domain of interest is split into the two regions, hold 4 and hold 5. A fire is initiated in hold 4 and the calorimeter is placed in hold 5 and is radiatively heated by the common bulkhead. Two additional compartments are included in the model to help simulate heat losses from the fire compartment. These are located to the forward (left in Fig. 8) of hold 4 and beneath hold 4 and have identical dimensions to hold 4. Holds 4 and 5 span the entire width of the ship and 298 K temperature boundary conditions are imposed on the external side of the port and starboard hulls as well to the weather deck immediately above. The height of all compartments in these tests is 3.7 m. The thickness' of the bulkheads, decks and overheads are summarised in Table 2.

Table 2. Thickness' of ship walls.

Location	Thickness (mm)
Starboard Hull	18.1
Port Hull	19.4
Bulkhead between Holds 4 and 5	8.2
Overhead	10.7
Holds 4 and 5 Deck	10.7
King Post	34.9

Between holds 4 and 5 is a large King Post which was once used to support a cargo crane. It is a thermally massive object and its effects have been included in the analysis. A representative part of the common bulkhead has been designated as the King Post and given a different mass. It receives an amount of radiation and convection from the fire compartment in proportion to its area. This amount is not available to the common bulkhead. The ordnance radiation model has also been modified to include the effects of the King Post by using the calculated King post temperature projected onto the common bulkhead at the appropriate locations.

Various fire scenarios for the *MAYO-LYKES* experiments were studied by Koski et al. (1997a). These included Heptane spray fires, wood crib fires and diesel pool fires. In this report, the diesel pool fire case will be compared with the numerical model only. This is because the heptane spray fires were directed at the common bulkhead and impinged on the surface. This resulted in significant temperature variations (hot spots) along the common bulkhead which are difficult to simulate using the numerical model in its present form. Without knowing the temperature distribution of the common bulkhead, ordnance radiative heating is also difficult to determine. The heptane spray fires were intended to represent a galley fire. As the purpose of the code is to model shipboard hydrocarbon pool fires, the diesel case was modelled only. For this reason the wood crib fires were also not compared. The diesel fuel fire was modelled using the fuel evaporation mass flux value in Table 1. Heat release for the diesel fuel was assumed to be 37.77 MJ/kg.

The calorimeter consisted of a 1.52 m long tube, 610 mm in diameter placed on the centreline of hold 5 parallel to the common bulkhead. The centre of the calorimeter was 2 m from the bulkhead and 0.4 m from the deck. Thermocouples were placed around the circumference of the calorimeter midway along its length and hence positioned midway along the common bulkhead. Heat transfer to the calorimeter was determined by Koski et al. (1997a) using a one-dimensional inverse heat conduction code where measured temperature distributions around the calorimeter can be converted to heat flux. Calibration techniques for this method (Koski et al. 1998) reveal that errors in determined heat flux depend on the simulation time as the one-dimensional model does not allow for circumferential heat flow. The error can vary from 1-20% depending on the time frame (1-60 minutes). Considerable noise is present on the presented heat flux data also. Considering these factors, an error of 13% was determined for the results quoted here. They were obtained at a simulation time of 20 minutes.

### 3.2.2 Comparison with Experimental Results

Figure 9 compares the experimental hold 4 (fire compartment) gas temperature with the numerical model. The thermocouple used for this comparison was at a considerable distance (5.1 m) away from the diesel fuel fire. The agreement can be considered good however, the model gas temperature rises too quickly in the initial part of the test. This difference cannot be accounted for.

Figure 10 compares the numerically modelled bulkhead temperature with those obtained from the experiment. The experimental results show two different temperatures depending on the position of the thermocouple. The thermocouple TC 5101 is positioned near the junction of the King Post and the common bulkhead. It may be that hot gas from the diesel fuel fire (which is directly behind the King Post) is jetting through a gap between the King Post and the common bulkhead and affecting the thermocouple response. The second thermocouple, TC 5102, is placed a considerable distance from the King Post and exhibits a response in closer agreement with the numerical model.

Figure 11 compares the experimentally measured calorimeter heat transfer with that predicted by the numerical model. To determine the radiative heating rate correctly, the measured calorimeter surface temperatures were used in the numerical model (see Eq. 11). As these were available for discrete angular positions only, a fourth order polynomial curve fit was used to obtain a continuous function of surface temperature with angle.

The experimental values represent the total heat transfer to the calorimeter and therefore include a convective component. The experimental points presented in Fig. 11 are modified by subtracting the convective component,

$$q_c = h_o(T_G - T_s) \quad (12)$$

where  $h_o$  is the ordnance convective heating rate and is assumed to be  $4.0 \text{ Wm}^{-2}\text{K}^{-1}$ . This value was determined from a value suggested by Holbrook and Crawley (1986) for heat transfer to ordnance suspended in hydrocarbon fuel fires. The hold 5 gas temperature,  $T_G$ , was obtained from the published measurements as were the calorimeter surface temperatures,  $T_s$ .

Figure 11 indicates that there is good agreement between the experimental results and the numerical model for ordnance heating rates. There are some discrepancies, however these may be due to the uneven spatial distribution of temperature across the common bulkhead during the experiments because of the presence of the King Post.



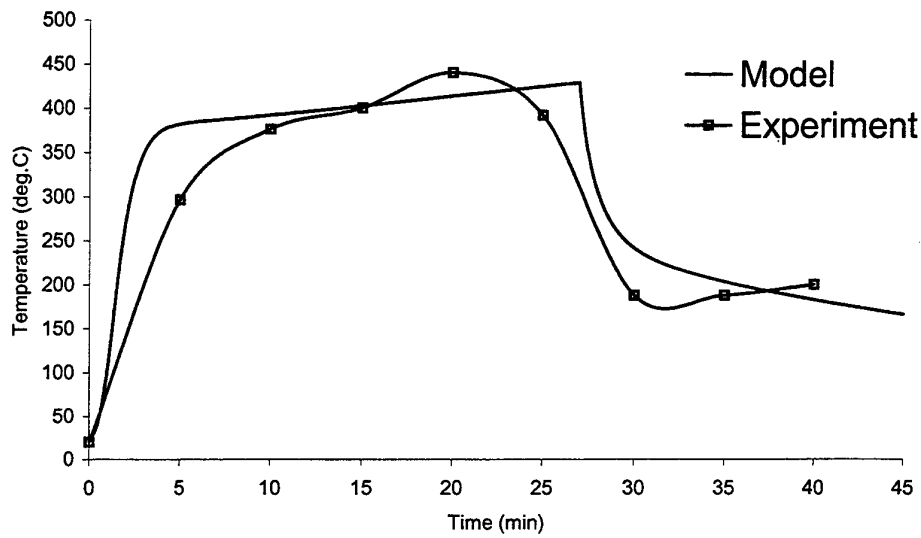


Figure 9. Comparison between experimental Hold 4 gas temperature and numerical model for Mayo-Lykes experiments.

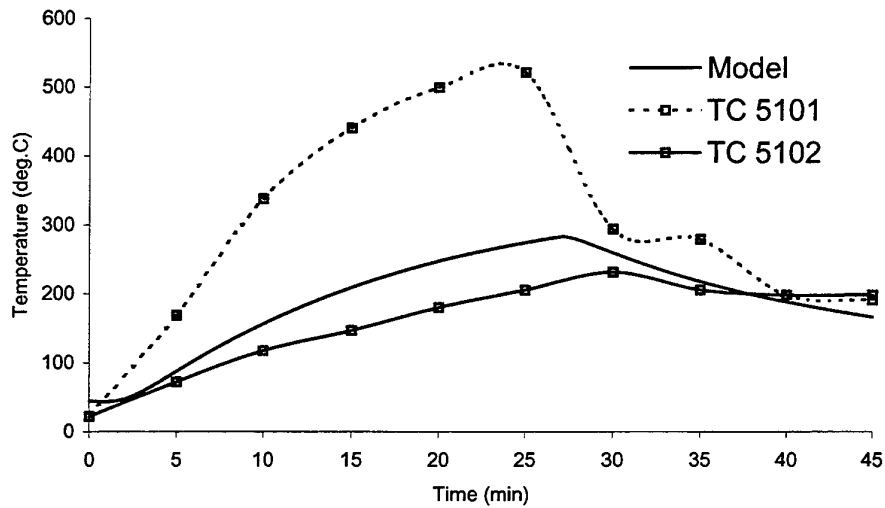


Figure 10. Comparison between experimental common bulkhead temperatures and numerical model for Mayo-Lykes experiments.

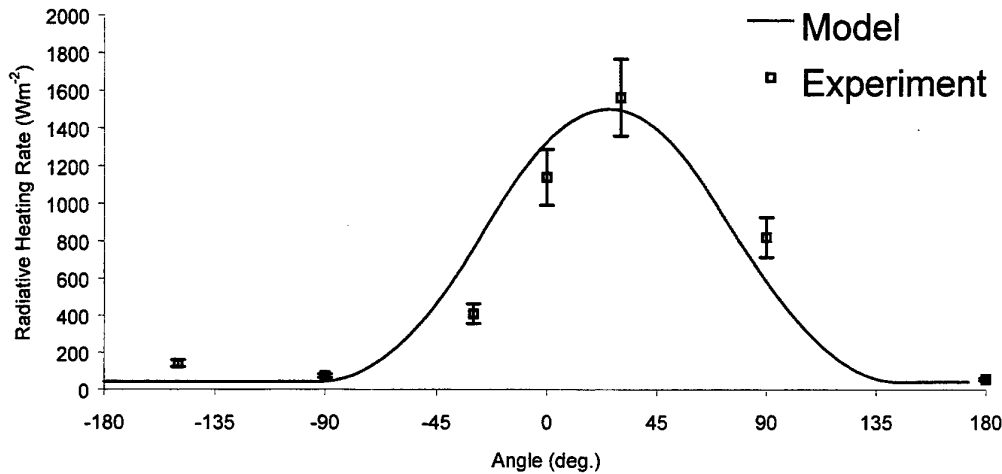


Figure 11. Comparison of computed radiative heating rates with experimentally measured values for the MAYO-LYKES.

### 3.3 Summary

It can be seen that for the test cases presented here, the numerical model provides reasonable agreement with published experimental results. The method of modelling the fire as heat release directly into the fire compartment gas appears appropriate for the level of detail required. The assumption of constant absorptivity ( $a = 0.01$ ) for the magazine gas is also justified. For radiative ordnance heating, the model provides reasonable comparison with experimental data. Certainly the level of agreement is adequate for the estimation of ordnance heating for cookoff studies.

## 4. Calculation of Ordnance Heating rates in the Anzac Air Weapons Magazine

The ANZAC class frigates utilise Sikorsky SH-60B "Seahawk" helicopters. Armaments for these helicopters are stored in the Air Weapons Magazine (AWM), located adjacent to the hanger area and forward of the landing deck. The two major ordnance items stored in the AWM are the Penguin anti-ship missile and the Mk46 air launched torpedo. In the present study, it is of interest to determine the heating rates to the Penguin missile rocket motor however the code can be used to determine heating rates to any cylindrically shaped object (ordnance) within the magazine.

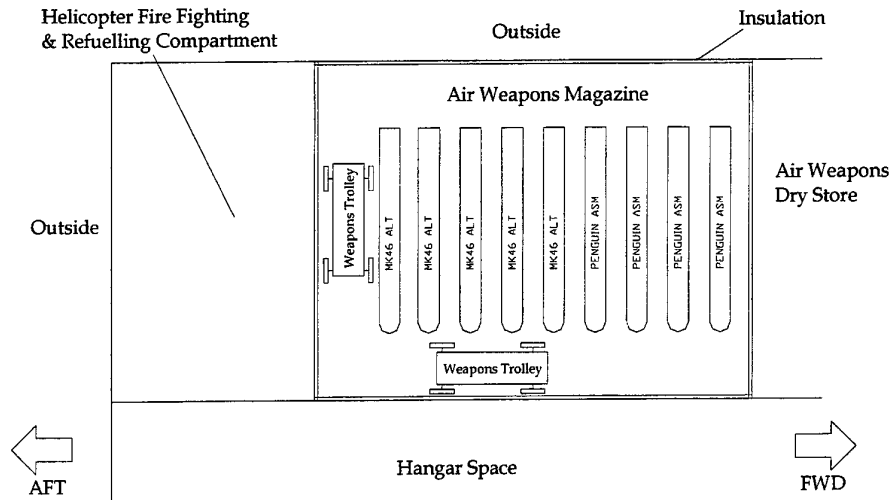


Figure 12. Plan view of ANZAC Air Weapons Magazine and adjacent compartments.

Figure 12 shows a schematic plan view of the AWM and the adjoining compartments. The ordnance is stored in the general arrangement as shown and are stacked three deep at each location. The ordnance can be moved by overhead crane onto the weapons trolley, which is indicated in typical positions. Immediately aft of the AWM is the helicopter fire fighting and refuelling compartment. On the port side is the outer bulkhead and beyond the inboard bulkhead is the hangar space. Forward of the AWM is the Air Weapons Dry Store where weapons fixtures such as canards are stored.

Two fire scenarios are considered in the present study. The first involves a hydrocarbon fuel fire in the refuelling compartment. A hydrocarbon fire may be initiated in this compartment by either a refuelling accident or through a liquid fuelled missile strike in this area. Any remaining fuel in the missile would be available to cause a post-flashover type fire in the area surrounding the impact. The second scenario involves a hydrocarbon fuel fire in the hangar space. Such a fire may occur if the fuel onboard the stowed helicopter were to ignite either due to an accident or combat situation.

The wall thickness' for the magazine are detailed in Table 3. The walls of the AWM are fitted with various types of insulation. The aft, outboard and inboard walls are covered with 50 mm thick mineral wool faced with 1mm steel sheet on the internal faces of the magazine. The forward bulkhead is fitted with 50 mm thick polyamide faced with 1mm steel sheet. Additional ablative insulation is provided to protect against possible rocket motor efflux in the case of an accidental motor firing. This region is located on the outboard bulkhead in the vicinity of the Penguin rocket motor exhaust.

*Table 3. Thickness' of ANZAC Air Weapons Magazine walls.*

Location	Thickness (mm)
Port Bulkhead	15
Inboard Starboard Bulkhead	7
Forward Bulkhead	4
Aft Bulkhead	4
Deck	7
Overhead	5

Modelling of the insulation requires some modifications to the way the numerical code functions. Figure 13 shows the construction used for the magazine insulation. It is assumed that the temperature varies linearly through the insulation between the bulkhead temperature and the steel sheet temperature. The heat conduction through the insulation is modelled using the relation,

$$q = k \frac{dT}{dx} \quad (13)$$

where  $k$  is the thermal conductivity for the insulation. The thermal conductivity of the insulation varies with insulation temperature. Durkin et al (1993) provide a relation for mineral wool insulation thermal conductivity,

$$k = \sigma \frac{16 T^3}{3 a_r} + k_o \quad (14)$$

where the constants  $a_r$  and  $k_o$  are  $461 \text{ m}^{-1}$  and  $0.0217 \text{ Wm}^{-1}\text{K}^{-1}$ , respectively. The temperature of the insulation used in Equation 14 is the mean of the linear distribution which is identical to the average of the bulkhead and steel sheet temperature.

The radiation heat transfer from the common bulkhead into the magazine is now replaced by the conduction term described by Equation 13. This heat transfer is now available to heat the steel sheet which increases in temperature and subsequently radiates into the magazine. Convection terms are still applied to the exposed surfaces of the bulkhead and steel sheet. Similar insulation models are applied to the other walls of the magazine. The polyamide insulation is assumed to have the same thermal conductivity properties as the mineral wool. Transient temperature measurements of polyamide and mineral wool (Durkin et al, 1993) show similar thermal performance when exposed to a post-flashover fire. During a simulation, the polyamide insulation experiences a mild (10-40 K) temperature rise and it was found that ordnance heating rates are very insensitive to its conductivity value. The effect of the additional ablative material near the Penguin rocket exhaust was ignored as it covered only a small area of the port bulkhead and would increase the model complexity unnecessarily.

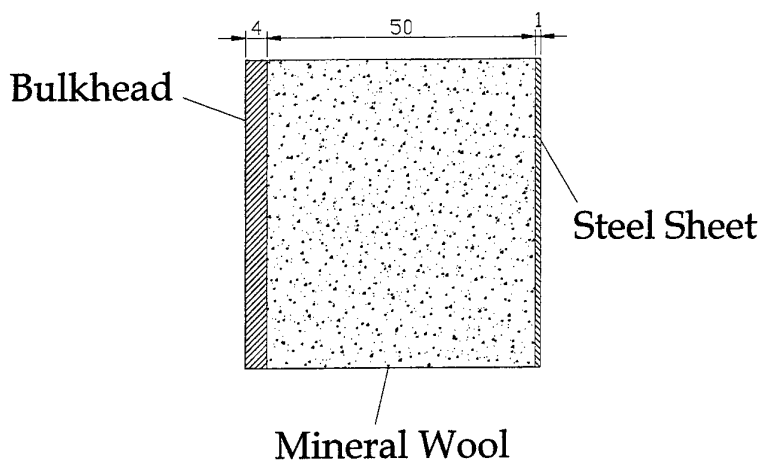


Figure 13. Representation of Air Weapons Magazine Insulation. Dimensions are shown for the aft bulkhead in millimetres.

#### 4.1 Test Case 1: Fire in Refuelling Compartment

A schematic of the geometry used in the model for this test case is shown in Fig. 14. The fire is situated in the refuelling bay and marked in Fig. 14 as the fire compartment. To model the heat losses from the fire compartment, upper and lower compartments are used. The dimensions of these compartments are similar to the actual compartments on upper and lower decks on the Anzac class frigates. Ambient air temperature boundary conditions are applied to the port, starboard and aft walls of the fire compartment. The starboard adjoining compartment is the hangar space and as this area is many times larger than the refuelling compartment it was decided to model this space as a constant temperature (298 K) boundary condition rather than add to the model complexity. Table 4 lists the dimensions of the various compartments used for test case 1.

Table 4. Compartment dimensions for test case 1.

Compartment	Dimensions (mm x mm x mm)
Fire Compartment	3000 x 4950 x 2900
Air Weapons Magazine	6500 x 4950 x 2900
Upper Compartment	3000 x 4950 x 2900
Lower Bulkhead	4500 x 4500 x 2900

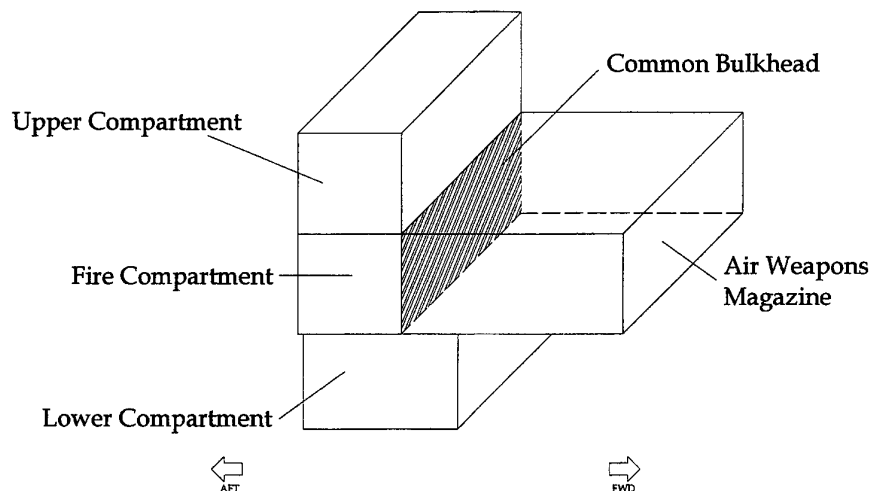


Figure 14. Schematic of geometry used for Anzac Air Weapons Magazine fire modelling. Test Case 1.

The fire was modelled as a hydrocarbon (Jet-A1) pool fire with a fixed surface area of 3 m<sup>2</sup>. This fire size was chosen as it resulted in a peak gas temperature of approximately 1500 K in the fire compartment. Experimentally simulated post-flashover fires (Durkin et al, 1993) measure similar gas temperatures and increasing system temperatures further than this would reduce the credibility of the model as the melting points of steel and the insulation are rapidly being approached.

Heat transfer to the Penguin missile was assessed in three separate locations. Two of these locations are in the ordnance racks where the missile is stored and the third position is on the weapons trolley, close to the common bulkhead. Table 5 lists the centreline positions of the missile for each position relative to the common bulkhead. Heat transfer is calculated around the circumference of the missile when the missile is parallel to the common bulkhead and at an axial position coincident with halfway along the length of the bulkhead. The nominal radius of the cylinder used to represent the Penguin missile was 0.155 m.

Table 5. Missile centreline positions used for ordnance heating calculations.

Position	Distance from deck (m)	Distance from Bulkhead (m)
1. Ordnance Rack	0.87	4.34
2. Ordnance Rack	0.87	1.59
3. Weapons Trolley	0.49	1.04

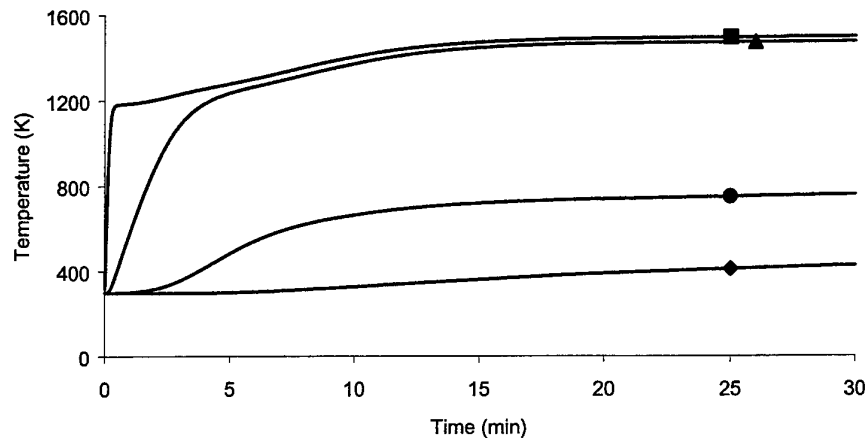


Figure 15. Transient temperature rise of various elements during test case 1. Symbols: ■ Fire compartment gas, ▲ Bulkhead, ● Steel sheet facing insulation, ◆ Magazine gas.

Figure 15 shows the predicted transient temperature rise of the fire compartment gas, bulkhead, steel sheet facing the insulation and the magazine gas temperature. For the 30 minute simulation, the fire compartment gas reaches an approximate steady state temperature of 1496 K. Due to the relatively thin bulkhead and the presence of the thermal insulation, the bulkhead reaches a similar temperature of 1473 K. The insulation ensures a significant lag in the temperature rise of the steel sheet. The approximate steady state temperature of the steel sheet is 756 K. The magazine gas reaches a maximum temperature of 424 K.

Figures 16-18 show the calculated radiative heating rates to the Penguin missile at the locations listed in Table 5. These heating rates are an incident radiative value only. No attempt is made to include a radiation loss due to the surface temperature of the missile as this is unknown at this stage. Future modelling using finite element heat transfer software would enable coupling of this value to the incident radiation flux for an accurate boundary condition. Convective heating rates are also not added due to the unknown transient missile surface temperature rise but can easily be done so during later modelling if it is calculated by finite element analysis.

The heating rates are greatly affected by the distance of the missile centreline to the heated common bulkhead. The maximum calculated heating rate is when the missile is located in the weapons trolley. The minimum calculated heating rate is when the missile is in position 1 in the ordnance rack. There is a factor of 3.6 difference between these two heating rates which illustrates the importance of ordnance position within the magazine when considering fire and heat transfer situations.

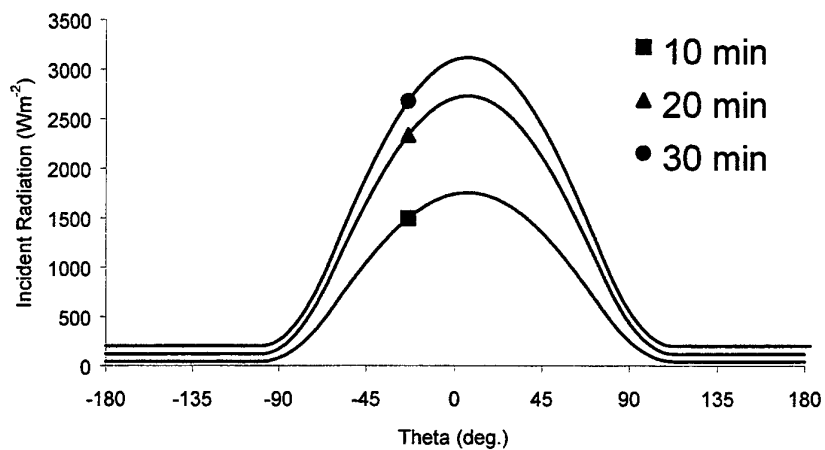


Figure 16. Radiative ordnance heating rates around Penguin missile for position 1 in the ordnance rack at various times.

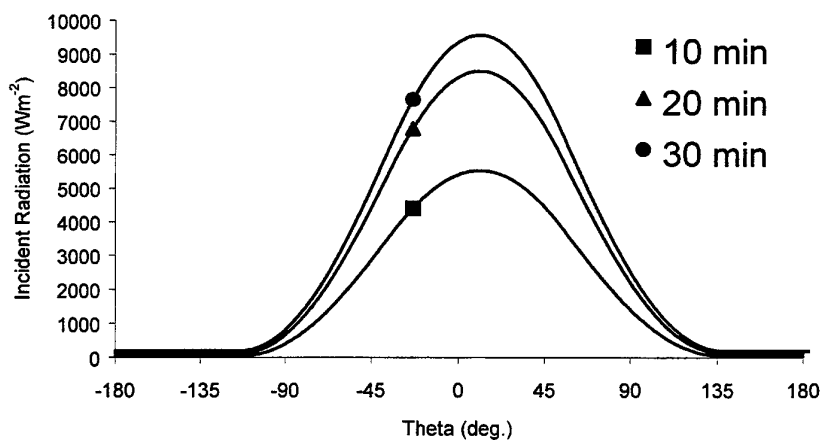


Figure 17. Radiative ordnance heating rates around Penguin missile for position 2 in the ordnance rack at various times.



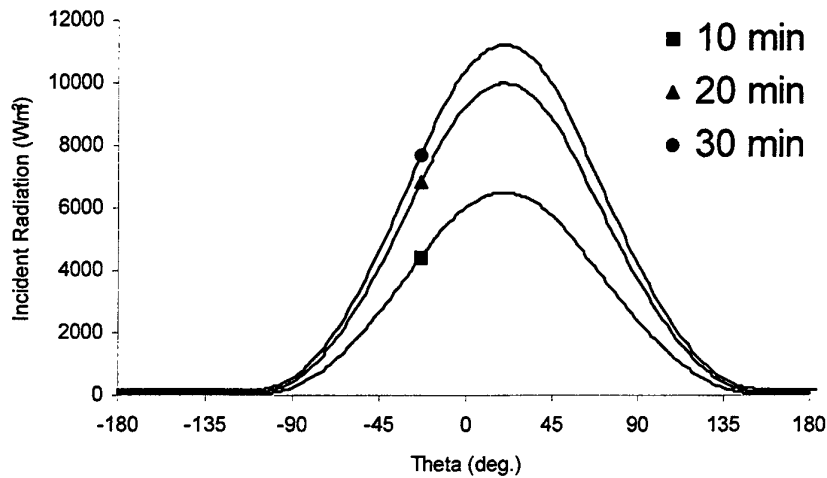


Figure 18. Radiative ordnance heating rates around Penguin missile for position 3 in the weapons trolley at various times.

## 4.2 Test Case 2: Fire in Hangar Space

Figure 19 is a schematic showing the geometry used to calculate heating rates when there is a fire in the hangar space. An important difference for this model is that the common bulkhead only forms part of the total hangar wall. An additional radiative heat loss term is included to account for the radiative loss from the hangar bulkhead in the area around the common bulkhead. This loss term was made proportional to the additional area and was calculated assuming this area was exposed to a 298 K boundary condition.

Three additional compartments are included in the model to simulate heat losses from the fire compartment. They are as shown in Fig. 19. Above and aft of the hangar are exposed to the atmosphere and 298 K boundary conditions are applied here. Table 6 summarises the dimensions used for test case 2.

Table 6. Compartment dimensions for test case 2.

Compartment	Dimensions (mm x mm x mm)
Fire Compartment	7100 x 14700 x 6000
Air Weapons Magazine	4950 x 6000 x 2900
Starboard Compartment	4950 x 14700 x 6000
Lower Compartment	7100 x 14700 x 2900
Forward Compartment	7100 x 2940 x 6000

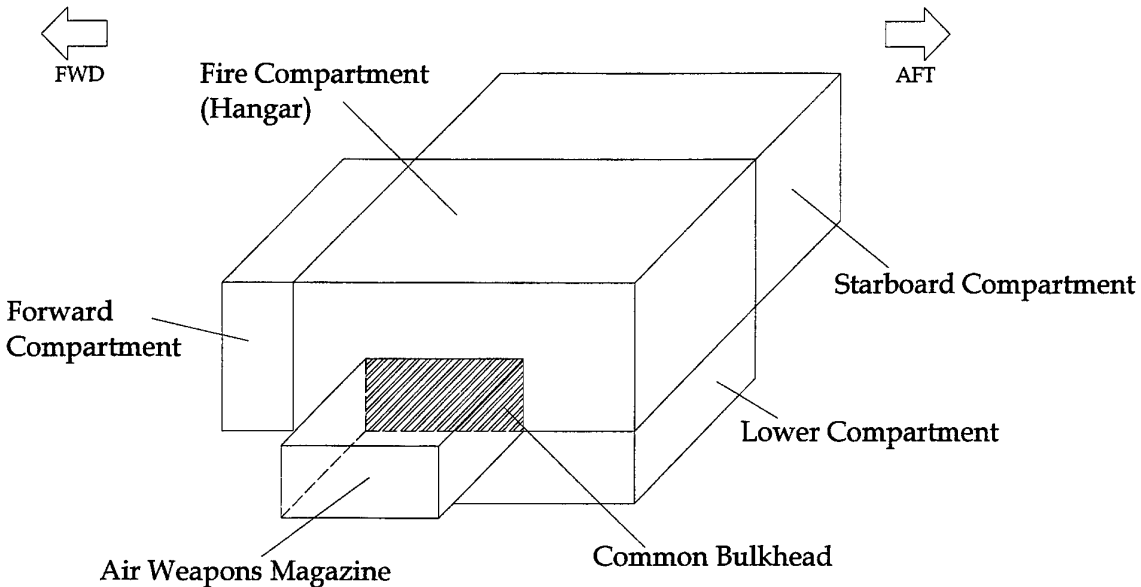


Figure 19. Schematic of geometry used for test case 2.

The fire is modelled as a 15 m<sup>2</sup> Jet-A1 hydrocarbon pool fire. The chosen nominal fire area is the approximate plan area of the Sikorsky SH-60B which was thought appropriate as this is the expected fuel source.

Figure 20 displays the calculated transient temperatures for the various elements for test case 2. The fire area is five times that of test case 1 however the bulkhead temperature rise is lower due to the volume of the hangar space. After the 30 minute simulation, the hangar space gas reaches a temperature of 1374 K while the bulkhead reaches 1179 K. The steel sheet which faces the insulation and heats the magazine reaches a temperature of 594 K. The magazine gas reaches a temperature 360 K.

Figure 21 presents incident radiative heating rates around the circumference of the Penguin missile at a location representative of when the missile is in the weapons trolley, next to the heated common bulkhead. The missile is placed parallel to the bulkhead with the axial location positioned midway along the bulkhead. The centreline of the missile is 490 mm from the deck and 1040 mm from the heated bulkhead. Despite the increase in fire size, the radiative heating rates are moderate when compared with the results of test case 1.

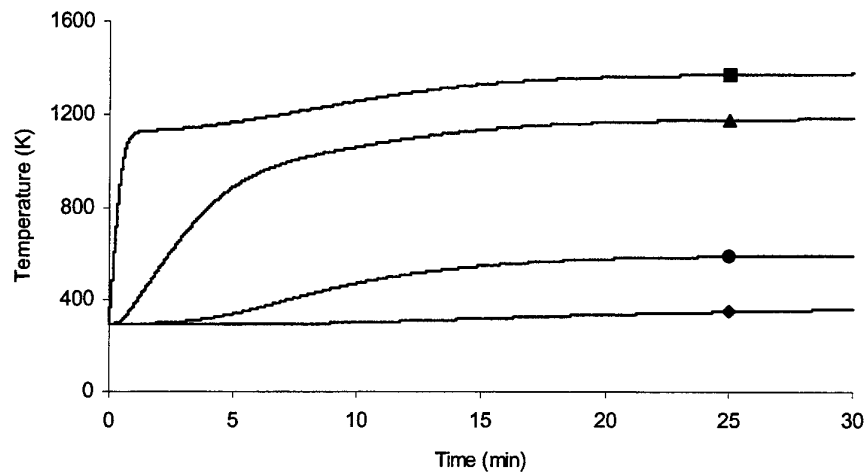


Figure 20. Transient temperature rise of various elements during test case 2. Symbols: ■ Fire compartment gas, ▲ Bulkhead, ● Steel sheet facing insulation, ◆ Magazine gas.

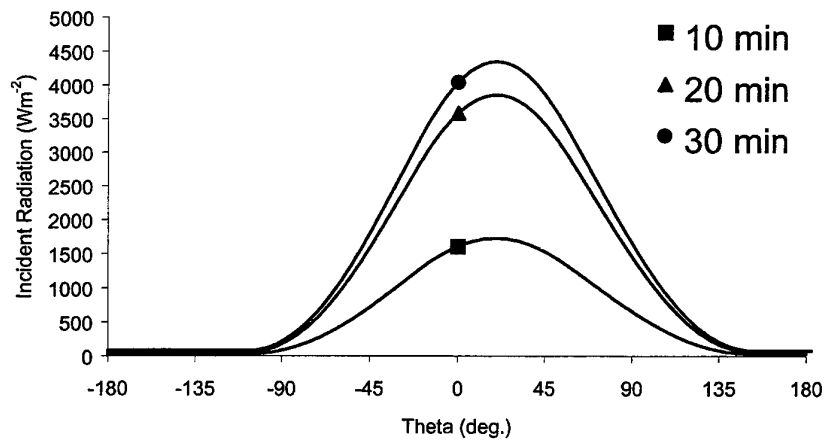


Figure 21. Radiative ordnance heating rates around Penguin missile for test case 2 at various times.

## 5. Conclusions and Future Work

This report has presented a numerical method which enables the determination of ordnance heating rates in shipboard magazines for the cases where the fire is in a compartment external to the magazine. The method uses an energy balance method for the explicit integration of the heat transmission equations. By comparing the results obtained from the numerical model with results found in the literature, it was concluded that the model provides results with reasonable accuracy for the prediction of heating rates to ordnance in shipboard magazines.

The model was used to provide transient, incident radiative heating rate information for the Penguin missile situated in various positions in the Anzac Air Weapons Magazine. Two fire scenarios were considered with fires in the refuelling compartment or in the hangar space. Results showed that maximum heating rates can vary markedly depending on the distance between the missile and the heated wall. For the results presented here, peak heating rates varied by a factor of 3.6 depending on position.

Now a reliable method to calculate ordnance heating rates has been determined, the results of the numerical model can be used to estimate time-to-reaction information in cookoff studies. Radiative heating rate information from this code can be used with a finite element representation of the Penguin rocket motor. A heat transfer analysis can then be run with the calculated surface temperature incorporated into the radiation boundary condition. Source terms for energetic material self heating can also be incorporated into the finite element code so as to determine the point where thermal runaway occurs. Coupling the radiation results from this report with a finite element model represents the next stage of the project for Weapons Systems Division and would provide Navy with valuable operational information for commanders and planners. The ability to calculate the time-to-reaction for shipboard ordnance in the situations presented in this report also reduces the requirement for full scale munitions cookoff testing representing significant cost benefits.

## 6. References

Croft, D.R. and Lilley, D.G. (1977) *Heat Transfer Calculations Using Finite Difference Equations*, Applied Science Publishers, London.

Durkin, A.F, Williams, F.W., Scheffy, J.L., Toomey, T.A., Hunt, S.P. and Darwin, R.L. (1993) *Post-Flashover Fires in Shipboard Compartments Aboard ex-USS Shadwell: Phase IV - Impact of Navy Fire Insulation*, Report NRL/MR/6183-93-7335, Naval Research Laboratory, U.S.A.

Holbrook, C.J. and Cawley, J.M. (1986) *A Liquid Fuel Fire Trial - Site Preparation at P&EE Port Wakefield and Test Fire November 1983*, Report WSRL-0435-TM, Weapons Systems Research Labortaory, Defence Science and Technology Organisation, Australia.

Holman, J.P. (1981) *Heat Transfer*, McGraw-Hill Book Company, Sydney.

Hottel, H.C. and Sarofim, A.F. (1967) *Radiative Heat Transfer*, McGraw-Hill Book Company, Sydney.

Johnson, H.T., Linley, L.J. and Mansfield, J.A. (1982) *Measurement of the Spatial Dependence of Temperature and Gas and Soot Concentrations within Large Open Hydrocarbon Fuel Fires*, Report NASA TM-58230, Lyndon B. Johnson Space Center, National Aeronautics and Space Administration, U.S.A.

Koski, J.A., Bobbe, J.G., Arviso, M., Wix, S.D., Beene, D.E., Byrd, R. and Graupmann, J. (1997a) *Experimental Determination of the Shipboard Fire Environment for Simulated Radioactive Material Packages*, Report SAND97-0506, Sandia National Laboratories, U.S.A.

Koski, J.A., Wix, S.D. and Cole, J.K. (1997b) *Calculation of Shipboard Fire Conditions for Radioactive Materials Packages with the methods of Computational Fluid Dynamics*, Report SAND97-2182, Sandia National Laboratories, U.S.A.

Koski, J.A., Wix, S.D. and Beene, D.E. (1998) *Experimental Measurement of a Shipboard Fire Environment with Simulated Radioactive Materials Packages, Very Large Scale Fires*, ASTM STP 1336, Keltner, N.R., Alvares, N.J. and Grayson, S.J. Eds., American Society for Testing and Materials.

Mansfield, J.A. (1996) *Preliminary Analysis of the Heating of Ordnance in Ship Magazines Due to a Fire in an Adjacent Compartment*, Report NAWC TP 8186, Naval Air Warfare Center Weapons Division China Lake, U.S.A.

Rossini, F.D., Pitzer, K.S., Arnett, R.L., Braun, R.M. and Pimentel, G.C. (1953) *Selected Values of Physical and Thermodynamic Properties of Hydrocarbons and Related Compounds*, American Petroleum Institute Project 44 Report, Carnegie Press, Pennsylvania.

Stull, V.R. and Plass, G.N. (1960) Emmissivity of Dispersed Carbon Particles, *Journal of the Optical Society of America*, Vol. 50, No. 2, pp121-129.

Victor, A.C. (1995) Simple Calculation Methods for Munitions Cookoff Times and Temperatures, *Propellants, Explosives, Pyrotechnics*, Vol 20, pp 252-259.

Williams, F.W., Back, G.G., Toomey, T.A., Ouellette, R.J., Scheffey, J.L. and Darwin, R.L. (1993) *Post-Flashover Fires in Shipboard Compartments Aboard ex-USS Shadwell: Phase III Venting of Large Shipboard Fires*, Report NRL/MR/6180-93-7338, Naval Research Laboratory, U.S.A.

## Appendix A: Shape Factor Equations

Radiative heat transfer between two walls within the magazine is controlled by the equation,

$$Q_{1,2} = \epsilon F_{1,2} A_1 \sigma T^4 \quad (A1)$$

where  $Q_{1,2}$  is the thermal radiation from area 1 to area 2,  $F_{1,2}$  is the radiation shape factor between area 1 and area 2,  $A_1$  is the area of area 1,  $\sigma$  is the stefan-boltzman constant and  $T$  is the temperature of area 1.

As the magazine is a rectangular prism, there are two shape factors which are relevant. The first is for radiation between two opposing walls and the second is between two walls in perpendicular planes. Theory described in Hottel and Sarofim (1967) describes how the shape factors can be derived. The equations used in the numerical model are listed here.

For two rectangles of equal dimensions ( $X$  wide and  $Y$  high), in parallel planes, directly opposed and separated by distance  $Z$ , the shape factor is,

$$F_{1,2} = \frac{1}{\pi} \left[ \frac{Z^2}{XY} \ln \frac{(X^2 + Z^2)(Y^2 + Z^2)}{(X^2 + Y^2 + Z^2)Z^2} - \frac{2Z}{Y} \tan^{-1} \frac{X}{Z} - \frac{2Z}{X} \tan^{-1} \frac{Y}{Z} \right. \\ \left. + \frac{2}{Y} \sqrt{Y^2 + Z^2} \tan^{-1} \frac{X}{\sqrt{Y^2 + Z^2}} \right. \\ \left. + \frac{2}{X} \sqrt{X^2 + Z^2} \tan^{-1} \frac{Y}{\sqrt{X^2 + Z^2}} \right] \quad (A2)$$

For two rectangles in perpendicular planes and having one common edge, the shape factor is given by equation A3. Figure A1 defines the terms,

$$F_{1,2} = \frac{1}{\pi XY} \left\{ \frac{1}{4} \ln \left[ \frac{(X^2 + Y^2 + Z^2)^{(Y^2 + Z^2 - X^2)} (Y^2)^{Y^2} (Z^2)^{Z^2}}{(X^2 + Y^2)^{(Y^2 - X^2)} (X^2 + Z^2)^{(Z^2 - X^2)} (Y^2 + Z^2)^{(Y^2 + Z^2)} (X^2)^{X^2}} \right] \right. \\ \left. + XY \tan^{-1} \frac{X}{Y} + XZ \tan^{-1} \frac{X}{Z} - X \sqrt{Y^2 + Z^2} \tan^{-1} \frac{X}{\sqrt{Y^2 + Z^2}} \right\} \quad (A3)$$

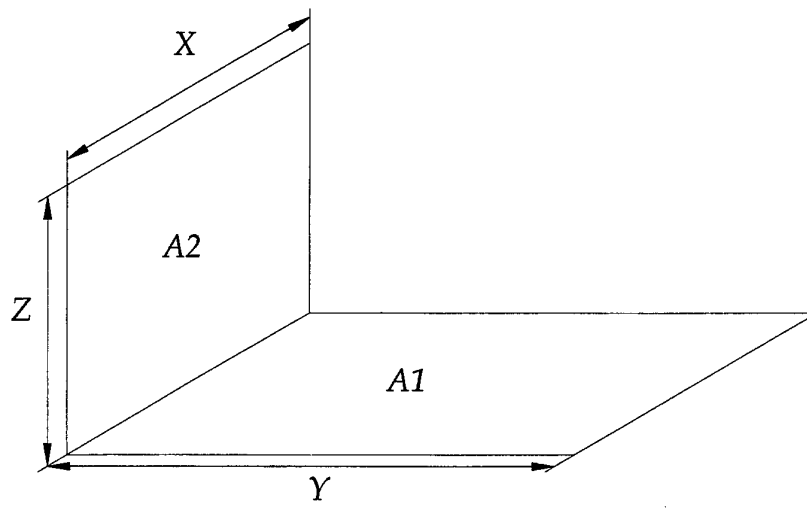


*Figure A1. Rectangles in perpendicular planes having one common edge.*



## DISTRIBUTION LIST

### Ordnance Heating Rates in Shipboard Magazines

Con Doolan

#### AUSTRALIA

##### DEFENCE ORGANISATION

###### Task Sponsor

DGNAVSYS

###### S&T Program

Chief Defence Scientist	}	shared copy
FAS Science Policy		
AS Science Corporate Management		
Director General Science Policy Development		
Counsellor Defence Science, London (Doc Data Sheet )		
Counsellor Defence Science, Washington (Doc Data Sheet )		
Scientific Adviser to MRDC Thailand (Doc Data Sheet )		
Scientific Adviser Policy and Command		
Navy Scientific Adviser		
Scientific Adviser - Army (Doc Data Sheet and distribution list only)		
Air Force Scientific Adviser		
Director Trials		

###### Aeronautical and Maritime Research Laboratory

Director

Chief of Weapons Systems Division

Research Leader

RLMWS Dave Thomson

Head (where appropriate)

HPST Sook Ying Ho

Task Manager

Con Doolan

Author(s):

Con Doolan (3 Copies)

###### DSTO Library and Archives

Library Fishermans Bend (Doc Data Sheet )

Library Maribyrnong (Doc Data Sheet )

Library Salisbury

Australian Archives

Library, MOD, Pyrmont (Doc Data sheet only)

US Defense Technical Information Center, 2 copies

UK Defence Research Information Centre, 2 copies

Canada Defence Scientific Information Service, 1 copy

NZ Defence Information Centre, 1 copy

National Library of Australia, 1 copy

###### Capability Systems Staff

Director General Maritime Development

Director General Aerospace Development (Doc Data Sheet only)

**Knowledge Staff**

Director General Command, Control, Communications and Computers (DGC4)  
(Doc Data Sheet only)  
Director General Intelligence, Surveillance, Reconnaissance, and Electronic Warfare (DGISREW) R1-3-A142 CANBERRA ACT 2600 (Doc Data Sheet only)  
Director General Defence Knowledge Improvement Team (DGDKNIT)  
R1-5-A165, CANBERRA ACT 2600 (Doc Data Sheet only)

**Navy**

SO (SCIENCE), COMAUSNAVSURFGRP, BLD 95, Garden Island, Locked Bag 12, PYRMONT NSW 2009 (Doc Data Sheet and distribution list only)  
LCDR Adrian O'Donoghue, Armament Section (Explosive Ordnance Systems), Directorate of Naval Weapons Systems, CP4-7-159  
Campbell Park Offices Canberra ACT 2600

**Army**

Stuart Schnaars, ABCA Standardisation Officer, Tobruk Barracks, Puckapunyal, 3662(4 copies)  
SO (Science), Deployable Joint Force Headquarters (DJFHQ) (L), MILPO Gallipoli Barracks, Enoggera QLD 4052 (Doc Data Sheet only)  
NPOC QWG Engineer NBCD Combat Development Wing, Tobruk Barracks, Puckapunyal, 3662 (Doc Data Sheet relating to NBCD matters only)

**Intelligence Program**

DGSTA Defence Intelligence Organisation  
Manager, Information Centre, Defence Intelligence Organisation

**Corporate Support Program**

Library Manager, DLS-Canberra

**UNIVERSITIES AND COLLEGES**

Australian Defence Force Academy  
Library  
Head of Aerospace and Mechanical Engineering  
Serials Section (M list), Deakin University Library, Geelong, 3217  
Hargrave Library, Monash University (Doc Data Sheet only)  
Librarian, Flinders University

**OTHER ORGANISATIONS**

NASA (Canberra)  
AusInfo

**OUTSIDE AUSTRALIA****ABSTRACTING AND INFORMATION ORGANISATIONS**

Library, Chemical Abstracts Reference Service  
Engineering Societies Library, US  
Materials Information, Cambridge Scientific Abstracts, US  
Documents Librarian, The Center for Research Libraries, US

**INFORMATION EXCHANGE AGREEMENT PARTNERS**

Acquisitions Unit, Science Reference and Information Service, UK

Library - Exchange Desk, National Institute of Standards and Technology, US

SPARES (5 copies)

**Total number of copies:      48**

<b>DEFENCE SCIENCE AND TECHNOLOGY ORGANISATION</b> <b>DOCUMENT CONTROL DATA</b>					
				1. PRIVACY MARKING/CAVEAT (OF DOCUMENT)	
2. TITLE Ordnance Heating Rates in Shipboard Magazines			3. SECURITY CLASSIFICATION (FOR UNCLASSIFIED REPORTS THAT ARE LIMITED RELEASE USE (L) NEXT TO DOCUMENT CLASSIFICATION)  Document (U) Title (U) Abstract (U)		
4. AUTHOR(S) Con Doolan			5. CORPORATE AUTHOR Aeronautical and Maritime Research Laboratory 506 Lorimer St Fishermans Bend Vic 3207 Australia		
6a. DSTO NUMBER DSTO-TR-1188		6b. AR NUMBER AR-011-953		6c. TYPE OF REPORT Technical Report	
7. DOCUMENT DATE July 2001					
8. FILE NUMBER J 9505/19/226		9. TASK NUMBER NAV 00/107		10. TASK SPONSOR DGNAVSYS	
				11. NO. OF PAGES 34	
				12. NO. OF REFERENCES 13	
13. URL on the World Wide Web <a href="http://www.dsto.defence.gov.au/corporate/reports/DSTO-TR-1188.pdf">http://www.dsto.defence.gov.au/corporate/reports/DSTO-TR-1188.pdf</a>				14. RELEASE AUTHORITY Chief, Weapons Systems Division	
15. SECONDARY RELEASE STATEMENT OF THIS DOCUMENT  <p style="text-align: center;"><i>Approved for public release</i></p>					
OVERSEAS ENQUIRIES OUTSIDE STATED LIMITATIONS SHOULD BE REFERRED THROUGH DOCUMENT EXCHANGE, PO BOX 1500, SALISBURY, SA 5108					
16. DELIBERATE ANNOUNCEMENT No Limitations					
17. CASUAL ANNOUNCEMENT Yes					
18. DEFTEST DESCRIPTORS Munitions storage, Magazines (ordnance), Heat transfer, Ship fires, Antiship missiles					
19. ABSTRACT This report describes a numerical method of determining the heating rate to ordnance cylinders stored in a Ship's Magazine. The source of heating is assumed to be a hydrocarbon fuel fire burning in an adjacent compartment. The heat released from the fire raises the temperature of a common bulkhead which then radiates energy onto the ordnance in the magazine. The method compares well with data available in the literature for shipboard fuel fire. Based on the strength of these comparisons, the method is used to estimate the likely heating rate for the Penguin ASM while mounted within the ANZAC Air Weapons magazine.					